# Low-Complexity CRB Minimization for ISAC with A Generalized Target Response Matrix

Shayan Zargari, Diluka Galappaththige, and Chintha Tellambura

***Abstract*—This paper presents a beamforming design for integrated sensing and communication (ISAC) systems using Riemannian manifold optimization to minimize the Cramér-Rao bound (CRB) of a generic target response matrix (TRM) for improving target estimation. CRB optimization is a challenging non-convex problem involving matrix inversion and its complex dependence on system parameters (e.g., beamforming, number of antennas, and number of targets), resulting in high dimensionality and the need to balance sensing accuracy and communication quality. Traditional solutions to these challenges, such as relaxed semidefinite programming (RSDP) and sequential convex cone optimization (SCCO), are computationally complex and have slow convergence. Thus, we propose a Riemannian conjugate iterative augmented Lagrangian manifold (RC-IALM) algorithm to minimize the TRM's CRB while ensuring communication quality. Numerical results demonstrate its superior computational efficiency and reduced running time. For instance, it is $33$ and $12$ times, respectively, faster than RSDP and SCCO benchmarks when there are $24$ transmit/receiver antennas at the base station.**

***Index Terms*—Integrated sensing and communication, Cramér-Rao bound, Beamforming, Manifold optimization.**

## I. Introduction

In radar signal processing, the target response matrix (TRM) represents how a radar system perceives a target based on its scattering characteristics, including reflection, absorption, and re-radiation of transmitted signals. It is advantageous in multiple-input multiple-output (MIMO) and synthetic aperture radar (SAR) applications, mapping transmitter-receiver responses to enable accurate target characterization in integrated sensing and communication (ISAC) [1], [2], [3]. The TRM manages diverse sensing scenarios without requiring prior channel knowledge and can be used with the Cramér-Rao bound (CRB) for beamforming designs. The CRB provides a lower bound on estimation error for key parameters such as range, velocity, and angle [4].

However, designing efficient beamforming strategies for optimizing the CRB of the TRM is challenging due to computational limitations and scalability issues. Existing methods such as relaxed semidefinite programming (RSDP) and sequential convex cone optimization (SCCO) suffer from high computational complexities $O(K^{0.5}N_t^6)$ and $O(K^{3.5}N_t^{6.5})$, respectively [2], limited scalability, and slow convergence [2], [5], [1]. These methods operate in high-dimensional Euclidean spaces and depend on relaxation techniques, such as semidefinite relaxation and rank-1 approximations, which compromise efficiency and optimality.

A brief overview of several prior works is as follows. Reference [2] minimizes the CRB of the TRM in MIMO ISAC systems while ensuring signal-to-interference-plus-noise ratio (SINR) constraints for communication users (CUs), employing RSDP and SCCO algorithms with Rank-1 approximation. Reference [6] proposes a per-user controllable waveform design for ISAC systems by leveraging a stacked-product Riemannian manifold to maximize radar SINR under per-user dynamic communication quality-of-service (QoS) constraints. However, it relies on fixed penalty weights for QoS enforcement, limiting convergence performance and constraint satisfaction under varying SINR requirements. Moreover, its sensing objective, i.e., radar SINR maximization, focuses on detection strength rather than estimation accuracy. In [7], a unified manifold optimization (MO) framework is proposed for pure radar systems, focusing on unimodular waveform and filter optimization with polarimetric power allocation. While it constructs a unified manifold space and employs a parallel conjugate gradient method for efficient computation, it does not address communication aspects, making it unsuitable for ISAC applications. Consequently, these limitations reduce the applicability of these prior works to generalized ISAC systems.

These limitations have prompted us to develop a more efficient ISAC beamforming framework using MO as it offers lower complexity and faster convergence rates [8], [9], [10]. MO eliminates the need for complex relaxation or approximations using adapted algorithms such as Riemannian conjugate (RC), steepest descent (SD), and others [8], [10], [9].

This work designs BS beamforming to minimize the CRB of TRM of a multi-CU, multi-target MIMO ISAC system while satisfying individual SINR constraints for CUs and transmit power budget. The objective function is augmented with a penalty term for violations of the SINRs. The proposed RC-iterative augmented Lagrangian manifold (IALM) algorithm iteratively adjusts optimization variables and Lagrange parameters to satisfy all constraints, unlike [6], which uses constant penalty weights. Compared to RSDP and SCCO [2], RC-IALM offers significantly lower computational complexity and execution time. For example, with $24$ transmit/receiver antennas and $4$ CUs, RC-IALM is $33$ and $12$ times faster than SCCO and RSDP, respectively, while restricting the search space to $\sim N_t^3$ dimensions.

## II. Preliminaries

This section describes the MIMO ISAC system, channel, and signal models.

*1) System Model:* A MIMO ISAC system is considered, comprising $N_t$ transmit antennas and $N_r$ receive antennas, serving $K$ downlink single-antenna CUs while simultaneously detecting targets as a monostatic radar. The BS antenna array is a uniform linear array (ULA) with antenna spacing $d$.

S. Zargari, D. Galappaththige, and C. Tellambura are with the Department of Electrical and Computer Engineering, University of Alberta, Edmonton, AB T6G 1H9, Canada (e-mail: {zargari, diluka.lg, ct4}@ualberta.ca).

*2) Channel Models:* The sensing channel is characterized by the TRM, denoted as $\mathbf{\Gamma} \in \mathbb{C}^{N_r \times N_t}$ [2], [1]. Specifically, $\mathbf{\Gamma}$ is treated as an unstructured matrix that contains information about the target and is estimated directly from the echo signal as an unknown variable [1]. Various sensing scenarios correspond to distinct structures of the TRM models. The following are two well-known models [11]:

- *Extended target model*: Radar detects a large object that spans multiple angles within a single range-Doppler bin. The TRM is expressed as $\mathbf{\Gamma} = \sum_{i=1}^{N_{\text{sc}}} \alpha_i \boldsymbol{\beta}(\theta_i)\boldsymbol{\alpha}^{\text{H}}(\theta_i)$, where $N_{\text{sc}}$ denotes the number of scatterers, $\alpha_i$ and $\theta_i$ represent the reflection coefficient and angle of the $i$-th scatterer, and $\boldsymbol{\alpha}(\theta)$ and $\boldsymbol{\beta}(\theta)$ are the transmit and receive steering vectors, respectively [11].
- *Point target model*: Radar detects multiple distinct point targets using OFDM waveforms. The TRM for the $n$-th subcarrier and $m$-th OFDM symbol is given by $\mathbf{\Gamma} = \boldsymbol{\beta}(\Theta)\mathbf{A}_n\mathbf{B}_m\boldsymbol{\alpha}^{\text{H}}(\Theta)$, where $\Theta$ represents the set of angles of scatterers. In addition, $\mathbf{A}_n$ and $\mathbf{B}_m$ account for phase shifts due to time delays and Doppler effects, with $\Delta f$ and $T_{\text{OFDM}}$ denoting subcarrier spacing and OFDM symbol duration, respectively [12].

A detailed analysis of specific target models is left for future work. Therefore, a general TRM model $\mathbf{\Gamma}$ is employed in this study to maintain broader applicability, rather than restricting the discussion to particular target models.

The TRM $\mathbf{\Gamma}$ is thus modeled with i.i.d. Gaussian entries, zero mean, and unit variance, representing a Swerling 1 or 2 target model with Gaussian complex amplitudes or multiple Swerling-type point targets [11]. Using the central limit theorem (CLT), the complex path gain is Gaussian due to the many reflecting paths between the targets and the BS [2].

The CU channel is modeled as Rayleigh fading, given as $\mathbf{F} = [\mathbf{f}_1, \ldots, \mathbf{f}_K]^{\text{H}} \in \mathbb{C}^{K \times N_t}$. This channel matrix is assumed to be perfectly estimated and known to the BS[1].

*3) Signal Models:* The BS transmits signal $\mathbf{X}_{\text{sig}} = \mathbf{W}_{\text{isac}}\mathbf{S}_{\text{com}} \in \mathbb{C}^{N_t \times L}$, which is jointly designed for CUs and targets sensing. Here, $\mathbf{W}_{\text{isac}} \in \mathbb{C}^{N_t \times K}$ is the dual-functional beamformer to be designed, and $\mathbf{S}_{\text{com}} \in \mathbb{C}^{K \times L}$ contains $K$ unit-power data streams intended for CUs. In addition, $L > N_t > K$ represents the length of the radar pulse or communication frame. The data streams are presumed to be orthogonal to each other, satisfying $\frac{1}{L}\mathbf{S}_{\text{com}}\mathbf{S}_{\text{com}}^{\text{H}} = \mathbf{I}_K$ [2]. Thus, the sample covariance matrix of $\mathbf{X}_{\text{sig}}$ is defined as $\mathbf{C}_{\mathbf{X}_{\text{sig}}} = \frac{1}{L}\mathbf{X}_{\text{sig}}\mathbf{X}_{\text{sig}}^{\text{H}} = \mathbf{W}_{\text{isac}}\mathbf{W}_{\text{isac}}^{\text{H}}$. Upon transmitting $\mathbf{X}_{\text{sig}}$, the reflected echo signal matrix at the BS is given by

$$\mathbf{Y}_{\text{sen}} = \mathbf{\Gamma}\mathbf{X}_{\text{sig}} + \mathbf{Z}_{\text{sen}}, \tag{1}$$

where $\mathbf{Z}_{\text{sen}} \in \mathbb{C}^{N_r \times L}$ is the additive white Gaussian noise (AWGN) with independently distributed elements, i.e., $\mathcal{CN}(0, \sigma_{\text{sen}}^2)$. The same ISAC waveform $\mathbf{X}_{\text{sig}}$ is also transmitted to CUs. The received signal by the CUs is given as

$$\mathbf{Y}_{\text{com}} = \mathbf{F}\mathbf{X}_{\text{sig}} + \mathbf{Z}_{\text{com}}, \tag{2}$$

[1]Channel estimation and data transmission/sensing occur in two separate time slots per coherent interval. Thus, the first slot in each coherent interval is dedicated to channel state information (CSI) estimation [8]. Thus, CSI is available.

where $\mathbf{Z}_{\text{com}} \in \mathbb{C}^{K \times L}$ represents AWGN, with each element having a zero mean and variance of $\sigma_{\text{com}}^2$.

## III. System Performance and Problem Formulation

This section determines system performance using the CRB for the targets at the BS and the communication rates/SINRs at the CUs. Then, it formulates the problem for evaluating and optimizing the MIMO ISAC system setup.

*1) CRB for Target Sensing:* CRB is widely recognized as a lower bound on the variance of unbiased estimators in parameter estimation [13]. This work thus aims to minimize the CRB to reduce the target estimation error.

First, let us define $\boldsymbol{\nu} = \left[\text{vec}\left(\Re(\mathbf{\Gamma})^{\text{T}}\right), \text{vec}\left(\Im(\mathbf{\Gamma})^{\text{T}}\right)\right]^{\text{T}}$, where $\text{vec}(\cdot)$ is the vectorization operator. Then, we rewrite (1) as $\text{vec}\left(\mathbf{Y}_{\text{sen}}\right) = \text{vec}(\mathbf{\Gamma}\mathbf{X}_{\text{sig}}) + \text{vec}\left(\mathbf{Z}_{\text{sen}}\right) = \mathbf{\Phi}\,\text{vec}(\mathbf{\Gamma}) + \text{vec}(\mathbf{Z}_{\text{sen}})$, where $\mathbf{\Phi} \triangleq \mathbf{X}_{\text{sig}}^{\text{T}} \otimes \mathbf{I}_{N_r}$, where $\otimes$ is tensor product. Given that the noise $\mathbf{Z}_{\text{sen}}$ follows a Gaussian distribution, the Fisher information matrix (FIM) for $\boldsymbol{\nu}$ is given by

$$[\mathbf{\Sigma}]_{ij} = \frac{2}{\sigma_{\text{sen}}^2}\Re\left(\text{tr}\left(\frac{\partial\left(\mathbf{\Phi}\,\text{vec}\left(\mathbf{\Gamma}\right)\right)^{\text{H}}}{\partial\nu_i}\frac{\partial\mathbf{\Phi}\,\text{vec}\left(\mathbf{\Gamma}\right)}{\partial\nu_j}\right)\right), \tag{3}$$

where $\text{tr}(\cdot)$ is the trace operator, $\Re(\cdot)$ denotes the real part, $[\mathbf{\Sigma}]_{ij}$ denotes the $(i,j)$-th entry of $\mathbf{\Sigma}$, and $\nu_i$ is the $i$-th element of $\boldsymbol{\nu}$ [2]. Consequently, one obtains

$$\mathbf{\Sigma} = \frac{2L}{\sigma_{\text{sen}}^2}\begin{bmatrix} \Re\left(\mathbf{C}_{\mathbf{X}_{\text{sig}}}^{\text{T}} \otimes \mathbf{I}_{N_r}\right) & -\Im\left(\mathbf{C}_{\mathbf{X}_{\text{sig}}}^{\text{T}} \otimes \mathbf{I}_{N_r}\right) \\ \Im\left(\mathbf{C}_{\mathbf{X}_{\text{sig}}}^{\text{T}} \otimes \mathbf{I}_{N_r}\right) & \Re\left(\mathbf{C}_{\mathbf{X}_{\text{sig}}}^{\text{T}} \otimes \mathbf{I}_{N_r}\right) \end{bmatrix}, \tag{4}$$

where $\Im(\cdot)$ denotes the imaginary part. Subsequently, the CRB for each parameter is derived as the diagonal elements of the inverse of $\mathbf{\Sigma}$.

It is notable that $\mathbf{X}_{\text{sig}} \in \mathbb{C}^{N_t \times L}$ is rank-deficient. As a result, transmitting only $K$ signal streams leaves insufficient freedom to fully recover the rank-$N_t$ matrix $\mathbf{\Gamma}$ [2]. Furthermore, $\mathbf{\Sigma}$ becomes singular, implying the non-existence of an unbiased estimator. Although constraining $\mathbf{\Gamma}$ to a subset and utilizing a modified CRB may address this issue, it inevitably leads to reduced target estimation performance due to limited radar flexibility. To ensure robust radar performance, $\mathbf{X}_{\text{sig}}$ is structured to maximize the available flexibility ($N_t$) by incorporating dedicated sensing streams in addition to the data streams intended for the CUs [2]. These sensing streams are dedicated solely to target sensing. The data matrix can be reexpressed as $\mathbf{S}_{\text{isac}} = [\mathbf{S}_{\text{com}}; \mathbf{S}_{\text{sen}}] \in \mathbb{C}^{N_t \times L}$, where $\mathbf{S}_{\text{sen}} \in \mathbb{C}^{(N_t-K)\times L}$ denotes the dedicated sensing streams, which are orthogonal to $\mathbf{S}_{\text{com}}$. Hence, for sufficiently large $L$, it holds that $\frac{1}{L}\mathbf{S}_{\text{isac}}\mathbf{S}_{\text{isac}}^{\text{H}} = \mathbf{I}_{N_t}$. Thus, the ISAC beamformer is redefined as $\mathbf{V}_{\text{isac}} = [\mathbf{W}_{\text{com}}, \mathbf{W}_{\text{sen}}] \in \mathbb{C}^{N_t \times N_t}$, where $\mathbf{W}_{\text{com}} = [\mathbf{w}_1, \ldots, \mathbf{w}_K] \in \mathbb{C}^{N_t \times K}$ and $\mathbf{W}_{\text{sen}} = [\mathbf{w}_{K+1}, \ldots, \mathbf{w}_{N_t}] \in \mathbb{C}^{N_t \times (N_t-K)}$ denote the communication and sensing beamformers, respectively. In this way, the transmitted signal $\mathbf{X}_{\text{sig}} = \mathbf{V}_{\text{isac}}\mathbf{S}_{\text{isac}}$ achieves full rank of $N_t$. In this ISAC signal model, the overall beamformer $\mathbf{V}_{\text{isac}}$ is employed to ensure target sensing accuracy, thereby maintaining unbiased estimation feasibility. The initial $K$ columns of $\mathbf{V}_{\text{isac}}$, denoted as $\mathbf{W}_{\text{com}}$, carry the information data for the CUs. As a result, the sample covariance matrix of $\mathbf{X}_{\text{sig}}$,

i.e., $\mathbf{C}_{\mathbf{X}_{\text{sig}}} = \mathbf{V}_{\text{isac}}\mathbf{V}_{\text{isac}}^{\text{H}}$. is now invertible, having a full rank of $N_t$. The CRB for estimating $\mathbf{\Gamma}$ is given as follows [2]:

$$\text{CRB}(\mathbf{\Gamma}) = \text{tr}\left(\mathbf{\Sigma}^{-1}\right) = \frac{\sigma_{\text{sen}}^2 N_r}{L}\,\text{tr}\left(\mathbf{C}_{\mathbf{X}_{\text{sig}}}^{-1}\right). \tag{5}$$

*2) Communication SINR:* CUs decode their intended data using the received signal from the BS. From (2), the received SINR at the $k$-th CU is given by

$$\gamma_k = \frac{|\mathbf{f}_k^{\text{H}}\mathbf{V}_{\text{isac}}\mathbf{E}_k|^2}{\sum_{i\in\tilde{\mathcal{N}}_t}|\mathbf{f}_k^{\text{H}}\mathbf{V}_{\text{isac}}\mathbf{E}_i|^2 + \sigma_{\text{com}}^2},\ \forall k \in \mathcal{K}, \tag{6}$$

where $\mathcal{K} \triangleq \{1,\ldots,K\}$, $\tilde{\mathcal{N}}_t \triangleq \mathcal{N}_t \setminus \{k\}$, $\mathbf{E} = \mathbf{I}_{N_t} \in \mathbb{R}^{N_t\times N_t}$, and $\mathbf{E}_k$ is the $k$-th column of $\mathbf{E}$.

*3) Problem Formulation:* Our primary goal is to minimize the target estimation CRB while adhering to constraints on communication performance, i.e., minimum SINR, and maximum BS transmit power by optimizing beamformer $\mathbf{V}_{\text{isac}}$. The optimization problem is formulated as

$$\mathbf{P}: \quad \min_{\mathbf{V}_{\text{isac}}}\ \text{tr}\left(\left(\mathbf{V}_{\text{isac}}\mathbf{V}_{\text{isac}}^{\text{H}}\right)^{-1}\right), \tag{7a}$$

$$\text{s.t} \quad \gamma_k \geq \gamma_k^{\text{th}},\ \forall k, \tag{7b}$$

$$\text{tr}\left(\mathbf{V}_{\text{isac}}\mathbf{V}_{\text{isac}}^{\text{H}}\right) \leq p_{\max}, \tag{7c}$$

where (7b) ensures the SINR required for each CU, in which $\gamma_k^{\text{th}}$ is the intended SINR threshold for the $k$-th CU, and (7c) sets the BS transmit power constraint, with a maximum allowable transmit power of $p_{\max}$.

## IV. Proposed Solution

Non-convex optimization problem $\mathbf{P}$ is solved using MO to determine the optimal BS beamforming. First, the power constraint is normalized to ensure $\text{tr}\left(\mathbf{V}_{\text{isac}}\mathbf{V}_{\text{isac}}^{\text{H}}\right) \leq 1$. Next, a modified matrix $\tilde{\mathbf{V}}_{\text{isac}}$ is introduced, satisfying the condition $\text{tr}(\tilde{\mathbf{V}}_{\text{isac}}\tilde{\mathbf{V}}_{\text{isac}}^{\text{H}}) = \text{tr}(\mathbf{V}_{\text{isac}}\mathbf{V}_{\text{isac}}^{\text{H}}) + ||\mathbf{z}||_2^2 = 1$, where $\tilde{\mathbf{v}}_n = [\mathbf{w}_n^{\text{T}}, z_n]^{\text{T}}$ for $n \in \mathcal{N}_t \triangleq \{1,\ldots,N_t\}$. Here, $\mathbf{z} = [z_1,\ldots,z_{N_t}]$ is an auxiliary vector introduced to simplify power normalization while preserving constraint (7c). This normalization results in a complex sphere manifold, defined as $\mathcal{M} = \{\tilde{\mathbf{V}}_{\text{isac}} \in \mathbb{C}^{(N_t+1)\times N_t} \mid \text{tr}(\tilde{\mathbf{V}}_{\text{isac}}\tilde{\mathbf{V}}_{\text{isac}}^{\text{H}}) = 1\}$. Consequently, $\mathbf{P}$ can be transformed into a constrained optimization problem on the manifold $\mathcal{M}$ given by

$$\mathbf{P}_1: \min_{\tilde{\mathbf{V}}_{\text{isac}}\in\mathcal{M}}\ g(\tilde{\mathbf{V}}_{\text{isac}}) = \text{tr}\left(\left(\tilde{\mathbf{V}}_{\text{isac}}\tilde{\mathbf{V}}_{\text{isac}}^{\text{H}}\right)^{-1}\right), \tag{8a}$$

$$\text{s.t}\ \ \Upsilon_k(\tilde{\mathbf{V}}_{\text{isac}}) = \gamma_k^{\text{th}} - \frac{|\hat{\mathbf{f}}_k^{\text{H}}\tilde{\mathbf{V}}_{\text{isac}}\mathbf{E}_k|^2}{\sum_{i\in\tilde{\mathcal{N}}_t}|\hat{\mathbf{f}}_k^{\text{H}}\tilde{\mathbf{V}}_{\text{isac}}\mathbf{E}_i|^2 + \sigma_{\text{com}}^2} \leq 0, \forall k, \tag{8b}$$

where $\hat{\mathbf{f}}_k = \sqrt{p_{\max}}[\mathbf{f}_k; 0] \in \mathbb{C}^{N_t+1\times 1}$ is adjusted to match the problem's dimensionality and scaling. In the Riemannian manifold $\mathcal{M}$, the functions $g(\tilde{\mathbf{V}}_{\text{isac}})$ and $\Upsilon_k(\tilde{\mathbf{V}}_{\text{isac}})$ are continuously differentiable from $\mathcal{M}$ to $\mathbb{R}$. However, problem $\mathbf{P}_1$ includes constraints (8b), which extends beyond the manifold limits. Fortunately, these constraints can be incorporated into the objective function as a penalty term by invoking the augmented Lagrangian model (ALM) [9]. Thus, the resulting Lagrangian function is given as

$$\mathcal{J}_\rho(\tilde{\mathbf{V}}_{\text{isac}}, \boldsymbol{\lambda}) = g(\tilde{\mathbf{V}}_{\text{isac}}) + \frac{\rho}{2}\sum_{k\in\mathcal{K}}\max\left\{0, \frac{\lambda_k}{\rho} + \Upsilon_k(\tilde{\mathbf{V}}_{\text{isac}})\right\}^2, \tag{9}$$

where $\rho > 0$ is a penalty parameter, and $\boldsymbol{\lambda} = [\lambda_1,\ldots,\lambda_K]^{\text{T}} \succeq 0 \in \mathbb{R}^{K\times 1}$ is the vector of Lagrange parameters [8], [9]. The ALM optimizes $\tilde{\mathbf{V}}_{\text{isac}}$ for a given $\boldsymbol{\lambda}$ by using the MO approach and updates $\boldsymbol{\lambda}$ with a gradient-based rule [14]. To apply ALM to Riemannian manifolds, the decision variable $\tilde{\mathbf{V}}_{\text{isac}}$ is constrained to a manifold $\mathcal{M}$. This constraint ensures that $\mathcal{J}_\rho(\tilde{\mathbf{V}}_{\text{isac}}, \boldsymbol{\lambda})$ remains differentiable with respect to $\tilde{\mathbf{V}}_{\text{isac}}$, allowing the ALM framework to be directly applied within the Riemannian context.

*1) Beamformer Design:* Optimization of (9) on the manifold $\mathcal{M}$ involves the following main steps [9], [8]:

- *Riemannian gradient*: The orthogonal projection of the Euclidean gradient $\nabla_{\tilde{\mathbf{V}}_{\text{isac}}^{(t)}}\mathcal{J}_\rho(\tilde{\mathbf{V}}_{\text{isac}}, \boldsymbol{\lambda})$ onto the tangent space $\mathcal{T}_{\tilde{\mathbf{V}}_{\text{isac}}^{(t)}}\mathcal{M}$ is given by $\text{grad}_{\tilde{\mathbf{V}}_{\text{isac}}^{(t)}}\mathcal{J}_\rho(\tilde{\mathbf{V}}_{\text{isac}}^{(t)}, \boldsymbol{\lambda}) = \nabla_{\tilde{\mathbf{V}}_{\text{isac}}^{(t)}}\mathcal{J}_\rho(\tilde{\mathbf{V}}_{\text{isac}}, \boldsymbol{\lambda}) - \tilde{\mathbf{V}}_{\text{isac}}^{(t)}\Re\{(\tilde{\mathbf{V}}_{\text{isac}}^{(t)})^{\text{H}}\nabla_{\tilde{\mathbf{V}}_{\text{isac}}^{(t)}}\mathcal{J}_\rho(\tilde{\mathbf{V}}_{\text{isac}}^{(t)}, \boldsymbol{\lambda})\}$, where $\mathcal{T}_{\tilde{\mathbf{V}}_{\text{isac}}^{(t)}}\mathcal{M} = \left\{\mathbf{c} \in \mathbb{C}^{(N_t+1)\times N_t} \mid \Re\{\text{tr}((\tilde{\mathbf{V}}_{\text{isac}}^{(t)})^{\text{H}}\mathbf{c})\} = 0\right\}$. Here, grad is gradient on a manifold, and $\nabla$ indicates Euclidean space gradient. Consequently, the Euclidean gradient of the objective function (9) is expressed by (10), where $\mathbf{1}_{\{x\}}$ is 1 if $x > 0$ and 0 otherwise.
- *Search direction and mapping*: Extending the Euclidean gradient method, MO uses search direction $\boldsymbol{\eta}^{(t+1)} = -\text{grad}_{\tilde{\mathbf{V}}_{\text{isac}}^{(t+1)}}\mathcal{J}_\rho(\tilde{\mathbf{V}}_{\text{isac}}, \boldsymbol{\lambda}) + \beta^{(t)}\mathcal{T}_{\tilde{\mathbf{V}}_{\text{isac}}^{(t)}\to\tilde{\mathbf{V}}_{\text{isac}}^{(t+1)}}(\boldsymbol{\eta}^{(t)})$, where $\boldsymbol{\eta}^{(t)}$ is the current search direction and $\beta^{(t)}$ is computed using the Hestenes-Stiefel approach [15]. Since $\boldsymbol{\eta}^{(t)}$ and $\boldsymbol{\eta}^{(t+1)}$ lie in different tangent spaces $\mathcal{T}_{\tilde{\mathbf{V}}_{\text{isac}}^{(t)}}\mathcal{M}$ and $\mathcal{T}_{\tilde{\mathbf{V}}_{\text{isac}}^{(t+1)}}\mathcal{M}$, a vector transport is necessary to connect them. This vector transport is defined as $\mathcal{T}_{\tilde{\mathbf{V}}_{\text{isac}}^{(t)}\to\tilde{\mathbf{V}}_{\text{isac}}^{(t+1)}}(\boldsymbol{\eta}^{(t)}) = \boldsymbol{\eta}^{(t)} - \tilde{\mathbf{V}}_{\text{isac}}^{(t+1)}\Re\{(\tilde{\mathbf{V}}_{\text{isac}}^{(t)})^{\text{H}}\boldsymbol{\eta}^{(t)}\}$. This approach ensures the search direction remains valid across different points on the manifold $\mathcal{M}$ [9], [8].
- *Retraction*: The RC-IALM algorithm transitions from the search direction $\boldsymbol{\eta}^{(t)}$ at the point $\tilde{\mathbf{V}}_{\text{isac}}^{(t)}$ to a new point on the manifold using a process called retraction. Retraction maps elements from the tangent space back to the manifold, ensuring the updated point remains on the manifold. This process is defined as $R_{\tilde{\mathbf{V}}_{\text{isac}}^{(t)}}(\alpha^{(t)}\boldsymbol{\eta}^{(t)}) = (\tilde{\mathbf{V}}_{\text{isac}}^{(t)} + \alpha^{(t)}\boldsymbol{\eta}^{(t)})/\|\tilde{\mathbf{V}}_{\text{isac}}^{(t)} + \alpha^{(t)}\boldsymbol{\eta}^{(t)}\|$, where $\alpha^{(t)}$ represents the step size.

Once $\tilde{\mathbf{V}}_{\text{isac}}$ is optimized, the Lagrangian multiplier vector $\boldsymbol{\lambda}$ is updated to assess the progress in satisfying the constraints.

*2) Lagrange Multiplier Tuning:* The update rule for the Lagrangian multiplier $\lambda_k$ at iteration $t$ is given by $\lambda_k^{(t+1)} = \text{clip}_{[\lambda_k^{\min},\lambda_k^{\max}]}\left(\lambda_k^{(t)} + \rho^{(t)}\Upsilon_k(\tilde{\mathbf{V}}_{\text{isac}}^{(t+1)})\right)$, where $\text{clip}_{[a,b]}(x) = \max\{a, \min(b,x)\}$ is the clip operator. Here, $\rho^{(t)} > 0$ is a penalty parameter. The clipping function limits each Lagrangian multiplier, $\lambda_k^{(t+1)}$, within the range $[\lambda_k^{\min}, \lambda_k^{\max}]$ [9].

$$\nabla_{\tilde{\mathbf{V}}_{\text{isac}}^{(t)}} \mathcal{J}_\rho(\tilde{\mathbf{V}}_{\text{isac}}, \boldsymbol{\lambda}) = -2\left(\left(\tilde{\mathbf{V}}_{\text{isac}}\tilde{\mathbf{V}}_{\text{isac}}^{\text{H}}\right)^{-1}\right)\left(\left(\tilde{\mathbf{V}}_{\text{isac}}\tilde{\mathbf{V}}_{\text{isac}}^{\text{H}}\right)^{-1}\right)\tilde{\mathbf{V}}_{\text{isac}} - 2\rho\sum_{k\in\mathcal{K}}\mathbf{1}_{\left\{\frac{\lambda_k}{\rho}+\Upsilon_k(\tilde{\mathbf{V}}_{\text{isac}})\right\}}\left(\frac{\lambda_k}{\rho}+\Upsilon_k(\tilde{\mathbf{V}}_{\text{isac}})\right)$$
$$\times\left(\frac{2\hat{\mathbf{f}}_k^{\text{H}}\tilde{\mathbf{V}}_{\text{isac}}^{(t)}\mathbf{E}_k\hat{\mathbf{f}}_k\mathbf{E}_k^{\text{H}}}{\sum_{j\in\tilde{\mathcal{N}}_t}\left|\hat{\mathbf{f}}_k^{\text{H}}\tilde{\mathbf{V}}_{\text{isac}}^{(t)}\mathbf{E}_j\right|^2+\sigma_{\text{com}}^2} - \sum_{i\in\tilde{\mathcal{N}}_t}\frac{2\left|\hat{\mathbf{f}}_k^{\text{H}}\tilde{\mathbf{V}}_{\text{isac}}^{(t)}\mathbf{E}_k\right|^2\hat{\mathbf{f}}_k^{\text{H}}\tilde{\mathbf{V}}_{\text{isac}}^{(t)}\mathbf{E}_i\hat{\mathbf{f}}_k\mathbf{E}_i^{\text{H}}}{\left(\sum_{j\in\tilde{\mathcal{N}}_t}\left|\hat{\mathbf{f}}_k^{\text{H}}\tilde{\mathbf{V}}_{\text{isac}}^{(t)}\mathbf{E}_j\right|^2+\sigma_{\text{com}}^2\right)^2}\right) \tag{10}$$

**Algorithm 1** : RC-IALM Algorithm

**Initialize**: $\tilde{\mathbf{V}}_{\text{isac}}^{(0)} \in \mathcal{M}$, $\boldsymbol{\lambda}^{(0)} \in \mathbb{R}^N$, $\epsilon_{\min}$, $\epsilon^{(0)} > 0$, $\rho^{(0)}$, $\theta_\epsilon \in (0,1)$, $\theta_\rho > 1$, $\{\lambda_k^{\min}, \lambda_k^{\max}\} \in \mathbb{R}$, $\tau \in (0,1)$, $\{\delta_1, \delta_2\} > 0$, set $t = 0$.
**while** $\text{dist}(g(\tilde{\mathbf{V}}_{\text{isac}}^{(t)}), g(\tilde{\mathbf{V}}_{\text{isac}}^{(t+1)})) \geq \delta_2$ or $\epsilon^{(t)} > \epsilon_{\min}$ **do**
  Update $\boldsymbol{\eta}^{(0)} = -\text{grad}_{\tilde{\mathbf{V}}_{\text{isac}}^{(0)}} \mathcal{J}_\rho(\tilde{\mathbf{V}}_{\text{isac}}, \boldsymbol{\lambda})$, set $t_1 = 0$.
  **while** $\|\text{grad}_{\tilde{\mathbf{V}}_{\text{isac}}^{(t_1)}} \mathcal{J}_\rho(\tilde{\mathbf{V}}_{\text{isac}}, \boldsymbol{\lambda})\|_2 > \delta_1$ **do**
    Perform line search to find $\alpha^{(t_1)}$.
    Update $\tilde{\mathbf{V}}_{\text{isac}}^{(t_1+1)}$ via $R_{\tilde{\mathbf{V}}_{\text{isac}}^{(t_1)}}(\alpha^{(t_1)}\boldsymbol{\eta}^{(t_1)})$.
    Update $\mathcal{T}_{\tilde{\mathbf{V}}_{\text{isac}}^{(t)} \to \tilde{\mathbf{V}}_{\text{isac}}^{(t_1+1)}}(\boldsymbol{\eta}^{(t_1)})$.
    Compute $\beta^{(t_1+1)}$ and update $\boldsymbol{\eta}^{(t_1+1)}$.
    $t_1 \leftarrow t_1 + 1$.
  **end while**
  Update the Lagrangian multiplier $\lambda_k^{(t+1)}, \forall k$.
  Set $\zeta_k^{(t+1)} = \max\left\{\frac{\Upsilon_k(\tilde{\mathbf{V}}_{\text{isac}}^{(t+1)})}{\lambda_k}, -\frac{\lambda_k^{(t+1)}}{\rho^{(t)}}\right\}, \forall k$.
  Adjust $\epsilon^{(t+1)} = \max\{\epsilon_{\min}, \theta_\epsilon \epsilon^{(t)}\}$.
  **if** $t = 0$ or $\max_k|\zeta_k^{(t+1)}| \leq \tau \max_k|\zeta_k^{(t)}|$ **then**
    $\rho^{(t+1)} = \rho^{(t)}$.
  **else**
    $\rho^{(t+1)} = \theta_\rho \rho^{(t)}$.
  **end if**
  $t \leftarrow t+1$, $\tilde{\mathbf{V}}_{\text{isac}}^{(0)} \leftarrow \tilde{\mathbf{V}}_{\text{isac}}^{(t+1)}$.
**end while**
**Output**: $\mathbf{V}_{\text{isac}}^* = \tilde{\mathbf{V}}_{\text{isac}}^*(1:N_t, N_t)$, $\boldsymbol{\lambda}^*$.

This ensures that the multipliers do not increase indefinitely, keeping the optimization process stable.

Algorithm 1 presents the RC-IALM algorithm for $\mathbf{P}$, which ensures convergence by iteratively refining the candidate solution. At each iteration $t$, a new candidate $\tilde{\mathbf{V}}_{\text{isac}}^{(t+1)}$ is generated, ensuring the Lagrangian value decreases or remains stable: $\mathcal{J}_\rho(\tilde{\mathbf{V}}_{\text{isac}}^{(t+1)}, \boldsymbol{\lambda}^{(t)}) \leq \mathcal{J}_\rho(\tilde{\mathbf{V}}_{\text{isac}}^{(t)}, \boldsymbol{\lambda}^{(t)}) + \epsilon^{(t)}$, where $\epsilon^{(t)} \to 0$. This guarantees that the solution approaches the global minimum. The penalty term $\rho^{(t)}$ controls convergence rate and constraint satisfaction [8]. Interested readers are referred to [9], [8] for the optimality and convergence properties of the proposed algorithm.

The computational complexities of MIMO-ISAC optimization methods vary greatly. RC-IALM is efficient with $O(N_t^3 + K^2N_t^2)$, making it suitable for large-scale systems. In comparison, RSDP has a higher complexity of $O(K^{0.5}N_t^6)$, and SCCO is the most complex at $O(K^{3.5}N_t^{6.5})$, limiting their scalability for large $N_t$ and $K$.

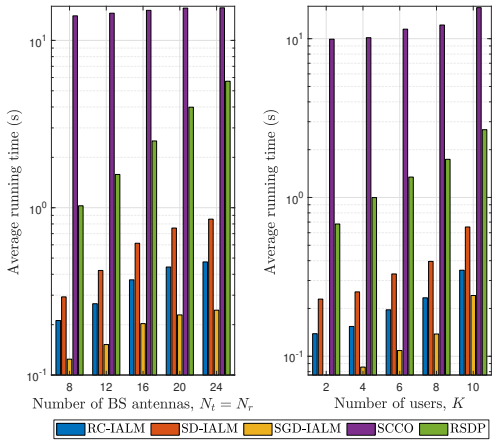


Fig. 1. Average running time vs. number of CUs and BS antennas for different algorithms.

## V. Simulation Results

This section evaluates the performance of RC-IALM. The BS is located at the origin, $\{0, 0\}$, and the CUs are randomly distributed within a $20\,\text{m}$ radius around $\{50, 30\}$. The simulation consists of $10^3$ Monte Carlo trials. The simulation parameters are set as follows [8], [9]: The carrier frequency is $3\,\text{GHz}$ and antenna spacing $d = \lambda/2$. The system has $N_t = N_r = 12$ antennas, $K = 4$ CUs, and $L = 30$. Maximum transmit power is $p_{\max} = 30\,\text{dBm}$, and noise variances $\{\sigma_{\text{sen}}^2, \sigma_{\text{com}}^2\}$ are $\{0, -80\}$ dBm. The tolerances are $\delta_1 = \delta_2 = 10^{-6}$. Initial and minimum accuracy tolerances are $\epsilon_0 = 10^{-3}$ and $\epsilon_{\min} = 10^{-6}$. Accuracy reduction $\theta_\epsilon$ and ratio $\tau$ set to 0.5, with $\rho_0 = 1$, $\theta_\rho = 4$. The SINR threshold is $1\,\text{dBm}$, and the Lagrange multiplier limits are $\{0, 10\}$.

RC-IALM is compared to the RSDP and SCCO methods [2]. For the RSDP benchmark, $\mathbf{P}$ is reformulated as an SDP by relaxing the rank-one constraint [2]. For the SCCO, the objective function of $\mathbf{P}$ is approximated using a first-order Taylor expansion, and (7b) is expressed as a SOCP constraint. Each solution is used in the next iteration until convergence. The optimization problems are solved using the CVX tool [16]. RC-IALM is also compared with SD-IALM and stochastic gradient (SGD)-IALM. The main difference lies in the update method: SD-IALM employs a basic SD direction, while SGD-IALM uses stochastic gradient updates, introducing randomness for potentially faster convergence.

Fig. 1 depicts the average running times of RC-IALM and benchmarks. The data are from Matlab simulation of an Intel® Core™ i7 processor, clocking at $2.50\,\text{GHz}$. As per Fig. 1, the execution time for all algorithms is proportional to $N_t$. However, the RC-IALM significantly outperforms SCCO and

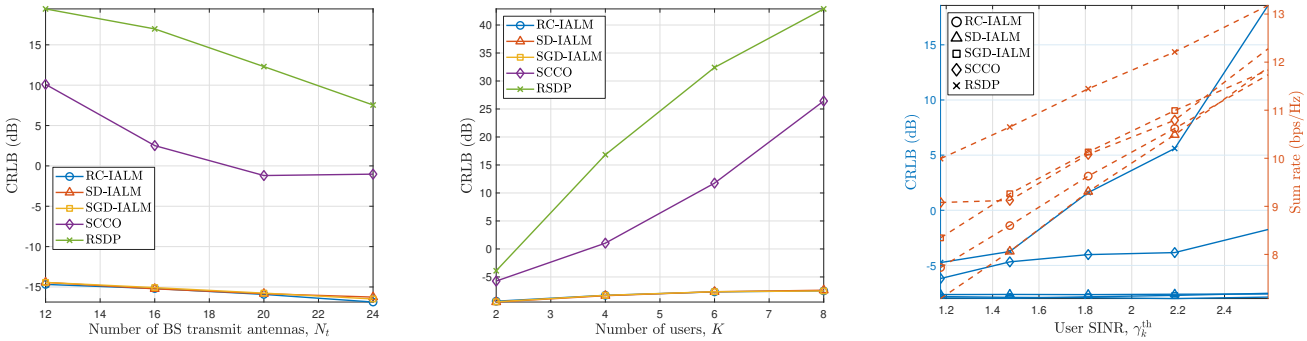


Fig. 2. Comparison of CRLB with respect to different algorithms. (a) CRLB vs. the number of BS antennas. (b) CRLB vs. the number of CUs. (c) CRLB and sum rate versus SINR thresholds, where solid lines represent the CRLB, while dashed lines indicate the sum rate.

RSDP. For example, with $N_t = 24$, RC-IALM reduces execution time by $96.97\,\%$ compared to SCCO and by $91.68\,\%$ compared to RSDP. It also shows a slight improvement of $44.53\,\%$ over SD-IALM, while SGD-IALM completes $48.52\,\%$ faster than RC-IALM. This occurs because RSDP and SCCO operate in the Euclidean space with $\sim N_t^6$ dimensions, while RC-IALM searches on a manifold with $\sim N_t^3$ dimensions. This reduction in search dimensions significantly decreases complexity. Second, RC-IALM directly translates non-convex $(\mathbf{P})$ into an MO problem without approximation. Compared to SGD-IALM, RC-IALM employs a conjugate gradient update method based on the Hestenes-Stiefel rule [15], ensuring more stable and deterministic convergence. In contrast, SGD-IALM utilizes stochastic gradient descent [17], which leads to less reliable convergence.

Fig. 2 shows the CRB performance of different algorithms as functions of (a) the number of BS antennas with $N_r = 12$, $\gamma_k^{\text{th}} = 5$, and $\frac{\text{CRB}(\mathbf{\Gamma})}{N_t - K}$ as the CRLB criterion (Fig. 2a), (b) the number of CUs with $\gamma_k^{\text{th}} = 5$ (Fig. 2b), and (c) the SINR threshold (Fig. 2c). Regardless of the simulation scenario, RC-IALM outperforms SCCO and RSDP. In Fig. 2a, RC-IALM surpasses SD-IALM by $1.25\,\%$ and SGD-IALM by over $2.5\,\%$ at $N_t = 20$. It also achieves a $91.75\,\%$ gain over SCCO and $176.875\,\%$ over RSDP, with continued superiority as the number of antennas increases. In Fig. 2b, RC-IALM, SD-IALM, and SGD-IALM maintain stable CRB performance as CU numbers grow, unlike SCCO and RSDP, which degrade. In Fig. 2c, RC-IALM remains stable across SINR thresholds, outperforming SCCO and RSDP, while achieving the highest sum rate gains.

## VI. Conclusion

This study developed a low-complexity beamforming algorithm, RC-IALM, for ISAC systems by minimizing the CRB of the TRM for target estimation while satisfying communication performance. Although the complexity of this problem increases exponentially with the number of antennas, RC-IALM reduces the search space from $N_t^6$ dimensions to a manifold of $N_t^3$, significantly lowering complexity. It achieves over $90\%$ faster convergence rate than conventional SCCO and RSDP methods due to its more efficient search directions and manifold structure, while demonstrating a stable CRB performance. Future work will focus on analyzing specific TRM models.

## References

[1] B. Tang and J. Li, "Spectrally constrained MIMO radar waveform design based on mutual information," *IEEE Trans. Signal Process.*, vol. 67, no. 3, pp. 821–834, Feb. 2019.

[2] F. Liu, Y.-F. Liu, C. Masouros, A. Li, and Y. C. Eldar, "A joint radar-communication precoding design based on Cramér-Rao bound optimization," in *Proc. IEEE Radar Conf.*, Mar. 2022, pp. 1–6.

[3] A. Hakimi, D. Galappaththige, and C. Tellambura, "A roadmap for NF-ISAC in 6G: A comprehensive overview and tutorial," *Entropy*, vol. 26, no. 9, Sept. 2024.

[4] J. A. Scheer, Ed., *Principles of Modern Radar: Basic Principles*, ser. Radar, Sonar and Navigation. Institution of Engineering and Technology, 2010.

[5] Z. He, W. Xu, H. Shen, Y. Huang, and H. Xiao, "Energy efficient beamforming optimization for integrated sensing and communication," *IEEE Wireless Commun. Lett.*, vol. 11, no. 7, pp. 1374–1378, Jul. 2022.

[6] D. An *et al.*, "Per-user dynamic controllable waveform design for dual function radar-communication system," *IEEE Trans. Aerosp. Electron. Syst.*, pp. 1–15, 2024.

[7] K. Zhong *et al.*, "Joint design of power allocation and unimodular waveform for polarimetric radar," *IEEE Trans. Geosci. Remote Sens.*, vol. 63, pp. 1–12, 2025.

[8] S. Zargari, D. Galappaththige, C. Tellambura, and H. Vincent Poor, "A Riemannian manifold approach to constrained resource allocation in ISAC," *IEEE Trans. Commun.*, pp. 1–1, 2024.

[9] C. Liu and N. Boumal, "Simple algorithms for optimization on Riemannian manifolds with constraints," *Appl. Math. Optim.*, vol. 82, pp. 949–981, Mar. 2020.

[10] S. Zargari, D. Galappaththige, C. Tellambura, and G. Y. Li, "Downlink beamforming for cell-free ISAC: A fast complex oblique manifold approach," *arXiv*, 2024.

[11] M. A. Richards, *Fundamentals of Radar Signal Processing*. McGraw-Hill Education, 2014.

[12] C. Sturm and W. Wiesbeck, "Waveform design and signal processing aspects for fusion of wireless communications and radar sensing," *Proc. IEEE*, vol. 99, no. 7, pp. 1236–1259, Jul. 2011.

[13] S. M. Kay, *Fundamentals of Statistical Signal Processing, Vol. I: Estimation Theory*. Englewood Cliffs, NJ, USA: Prentice Hall, 1998.

[14] E. G. Birgin and J. M. Martínez, *Practical Augmented Lagrangian Methods for Constrained Optimization*. Philadelphia, PA: Soc. Ind. Appl. Math., 2014.

[15] J. R. Shewchuk, "An introduction to the conjugate gradient method without the agonizing pain," USA, Tech. Rep., 1994. [Online]. Available: http://www.cs.cmu.edu/~quake-papers/painless-conjugate-gradient.pdf

[16] M. Grant and S. Boyd, "CVX: Matlab software for disciplined convex programming, version 2.1," 2014.

[17] N. Tripuraneni, N. Flammarion, F. R. Bach, and M. I. Jordan, "Averaging stochastic gradient descent on Riemannian manifolds," in *Ann. Conf. on Comput. Learn. Theor.*, 2018. [Online]. Available: https://api.semanticscholar.org/CorpusID:3645092